Computer Modeling in Engineering & Sciences

Tech Science Press

DOI: 10.32604/cmes.2022.019376

ARTICLE

Computational Investigation of Cell Migration Behavior in a Confluent Epithelial Monolayer

Jie Bai and Xiaowei Zeng*

Department of Mechanical Engineering, University of Texas at San Antonio, San Antonio, 78249, USA

*Corresponding Author: Xiaowei Zeng. Email: xiaowei.zeng@utsa.edu

Received: 20 September 2021 Accepted: 18 November 2021

ABSTRACT

Cell migration plays a significant role in many biological activities, yet the physical mechanisms of cell migration are still not well understood. In this study, a continuum physics-based epithelial monolayer model including the intercellular interaction was employed to study the cell migration behavior in a confluent epithelial monolayer at constant cell density. The epithelial cell was modeled as isotropic elastic material. Through finite element simulation, the results revealed that the motile cell was subjected to higher stress than the other jammed cells during the migration process. Cell stiffness was implied to play a significant role in epithelial cell migration behavior. Higher stiffness results in smaller displacement and lower migration speed.

KEYWORDS

Epithelial monolayer; cell migration; cell stiffness; intercellular interactions; finite element simulation

1 Introduction

Many biological activities such as embryogenesis [1–4], wound healing [5–7] and cancer metastasis [8–11] require collective cell migration in a coordinated way within a tissue [8,12–14]. Cells in these tissues are often densely packed together, and the motion of a cell is often strongly constrained by its neighbors [15]. When cellular movements are comparatively small, cellular rearrangements rarely happen, and cells are trapped by their immediate neighbors. Park et al. [16] performed a statistical analysis of these quasi-static collective cell motions which described such a cell layer to be solid-like and jammed. However, when cell movements are comparatively large in a cooperative way and swirling pattern, such a layer is described to be fluid-like and unjammed. The jammed to unjammed transition has been found in cancer metastasis, organogenesis, bronchial asthma, etc. [17]. Initiation of some biological processes such as tissue remodeling and wound repair require the quiescent cell layer to transit from jammed state to unjammed state via collective migration. During the cell migration process, the individual cell of the unjammed collective cells interacts with its neighbors cooperatively through chemical and mechanical cues. The cell jamming/unjamming transition is superficially similar to the epithelial-to-mesenchymal transition (EMT) which has also been shown to occur in wound healing. Although their distinctions

have been investigated [18], still little is known on unjammed-to-jammed transition for the densely packed cells.

Collective cell migration has received growing attention in recent studies which show that the cell migration behavior is governed by a set of parameters. Active motility, cell density, cell-cell interaction, cell shape, cell stiffness and applied stress are believed to be potential factors that can affect the collective cell migration behavior [19]. Experimental studies [16,20–22] have found that during collective cell migration, not only the leader cell may play an important role, but cell-cell adhesion forces may also influence the migratory behavior. By using the Monolayer Stress Microscopy, Park et al. [16] found that the jamming/unjamming transition in asthma is linked to cell shape change. As the layer becomes more unjammed, the cell shape changes from regular hexagonal to more elongated and more variable shape-like. It also showed the intercellular stresses are higher in unjammed bronchial epithelial cells from asthmatic donors compared with those in jammed cells from non-asthmatic donors. By studying the developing monolayers of human bronchial epithelial cells, Garcia et al. [23] found cell-cell contacts and cell-substrate contacts maturate with time, resulting in higher friction between cells that may influence the cell jamming/unjamming transition. Experiments have identified that intercellular adhesion force is regulated by proteins that resist and transmit forces at cell-cell junctions [12,24]. Studies have also shown that cell stiffness may also influence cell motility during the migration process [25–27].

On the other hand, researchers have used numerical tools of various complexity to investigate the collective cell migration behavior. The cellular Potts model (CPM) [28,29] was one of the early successful models. In the CPM [30,31], cells are considered as several sets of pixels that are updated by certain probabilistic rules. Different particle models [32–34] have been developed to study the collective cell motion in an epithelial sheet. It is found that both polarity-velocity alignment and locomotion interactions can affect the collective motion. Bi et al. [35,36] used a vertex model to describe the epithelial junctional and cortical tension rigidity transition in biological tissues. It was found that the onset of rigidity transition between liquid and solid was governed by a model parameter in confluent tissues. The self-propelled Voronoi (SPV) model was used to study the coherent motions in confluent cell monolayer sheets [37–39]. A cell-based FE model [40,41] was adopted to study the wound healing process. In this model, the cell-cell adhesion was represented by the tension force tangent to the cell edge. The simulation studies implied that either cell crawling or purse-string contraction can lead to wound closure. Lin et al. [42] proposed an interfacial interaction model to study the collective epithelial cell migration behavior. Through the simulation, it reveals that the direction of cell movement is better aligned with the local principal stress direction at the higher maximum shear stress region.

Although the collective cell migratory behaviors in confluent tissues have been studied, the mechanisms of coordinated motion in cells are still unclear and controversial due to the following attributes: First, there are limitations in experimental studies to identify individual contribution factor in the collective cell migration behavior; Second, the lack of advanced continuum physics-based computational tools also make it difficult to uncover the collective cell migration mechanism. Models such as the vertex model and particle model are advanced models. However, they are not real continuum physics-based models. How the mechanical clues will influence the collective cell migration behavior is not very clear. The model could not capture essential features of cell mechancial property and the intercellular interaction at cell-cell junction between adjacent cells. So it is necessary to develop continuum physics-based collective cell model to bridge the knowledge gap between cell biology and cell biomechanics in a confluent monolayer. In this study, a collective cell model considering intercellular adhesion, cell-substrate adhesion and cell stiffness,

is used to study the cell migration mechanism. An advanced computational model and finite element based simulation tool was developed to investigate how intercellular interaction and cell stiffness may affect the cell migration behavior.

2 Models and Materials

2.1 Geometric Model of the Epithelial Monolayer and Boundary Conditions

The epithelial monolayer is reported to be a thin layer of 3–15 μm in thickness [43,44]. For simplification, a 2D plane stress model of the epithelial monolayer was created using the Voronoi tessellation method to represent the monolayer sheet [35,45,46]. Generally, polygon-shaped epithelial cells were first generated within a square region using the Centroidal Voronoi tessellation method. Then, cell-cell interfacial zone was generated to characterise the intercelluar interaction between adjacent cells. In this study, sixty-four (64) densely packed epithelial cells were created and the average cell size was set to be around 30 μm, which is in the size range (10–36 μm) of epithelial cells [47]. The cell junction size was set to be 10 nm throughout the model, which was reported in literatures [48,49]. Fig. 1 illustrates the geometric configuration of the two-dimensional epithelial monolayer. The 64 cells in the simulation model are confined in the square box region, and the simulation box is fixed during the simulation. During the cell migration, the position of the centroid for each cell is updated, and thus the edges for each cell get updated. All cells are moving inside of the confined box.

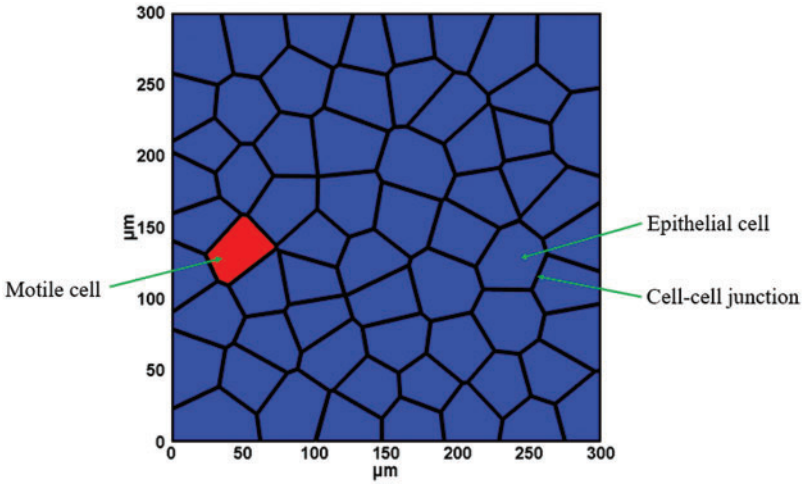

Figure 1: Geometry model of the epithelial monolayer sheet

2.2 Interaction Force Modeling

2.2.1 Intercellular Interaction Modeling at Cell-Cell Junction

The transmission of mechanical forces is broadly recognized to play a significant role during cell migration processes. While the motile cells move, they will interact with their neighboring cells, and the interaction force will be transmitted through cell-cell junctions [50]. Mechanical stresses exerted at cell-cell junctions have been studied in experiments with different measurements [51–54]. In experimental studies, the intercellular adhesion within a migrating monolayer can be decomposed into normal traction that is perpendicular to the cell-cell junction and shear traction that is tangential to the cell-cell junction as shown in Fig. 2.

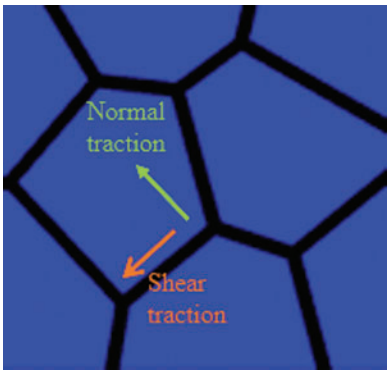

Figure 2: Intercellular interaction at cell-cell junction

Some computational frameworks such as the vertex model and cellular potts model have been developed to study the collective cell migration processes [29,35]. These models incorporate the contribution of the intercellular adhesion, however, they are pure mathematical models that could not capture the mechanical behavior of the cell tissue. In this study, the intercellular interactions at cell-cell junctions were modeled using an interfacial interaction model which was proposed by Lin et al. [42] to investigate the collective epithelial cell migration, and it takes the following forms:

$$F_n = \begin{cases} \sigma_{c-c}\left(\dfrac{d_n-\delta_0}{\delta_{dn}-\delta_0}\right)\left[e^{1-\dfrac{d_n-\delta_0}{\delta_{dn}-\delta_0}}\right]^{q_n} & d_n \le \delta_{dn} \\ \sigma_{c-c}\left(\dfrac{\delta_{fn}-d_n}{\delta_{fn}-\delta_{dn}}\right)^{p_n} & \delta_{dn} < d_n < \delta_{fn} \\ 0 & d_n \ge \delta_{fn} \end{cases} \tag{1}$$

$$F_t = \begin{cases} \tau_{c-c}\left(\dfrac{d_t}{\delta_{dt}}\right)\left[e^{\dfrac{1}{2}-\dfrac{d_t^2}{2\delta_{dt}^2}}\right]^{q_t} & 0 \le |d_t| \le \delta_{dt} \\ \tau_{c-c}\dfrac{d_t}{|d_t|}\left(\dfrac{\delta_{ft}-|d_t|}{\delta_{ft}-\delta_{dt}}\right)^{p_t} & \delta_{dt} \le |d_t| \le \delta_{ft} \\ 0 & |d_t| \ge \delta_{ft} \end{cases} \tag{2}$$

The traction-separation laws used to model the intercellular interaction is illustrated in Fig. 3. This model has been employed to describe intercellular interactions in collective cell migration and in other biological material modelings [42,55].

The critical intercellular interaction distance in both normal and tangential directions, δ_{dn} and δ_{dt} in our model, were estimated as 1 μm. The interaction cutoff distance in normal and tangential directions, δ_{fn} and δ_{ft}, were set as 2 μm. The intercellular adhesion strength in both normal and tangential directions, σ_{c-c} and τ_{c-c}, were approximated as 2 nN/μm^2 since the cell-cell adhesive traction were in a range of $1 \sim 8$ nN/μm^2 measured by Liu et al. [56]. The q_n and q_t describe the exponential behavior in the normal and tangential direction respectively, and were set to be one for simplificity. The p_n and p_t describe a type of linear detachment progression between adjacent

cells when the intercellular separation d_n or d_t exceeds δ_{dn} and δ_{dt} in the normal and tangential direction, respectively. The p_n and p_t were set to be one for simplificity in current study.

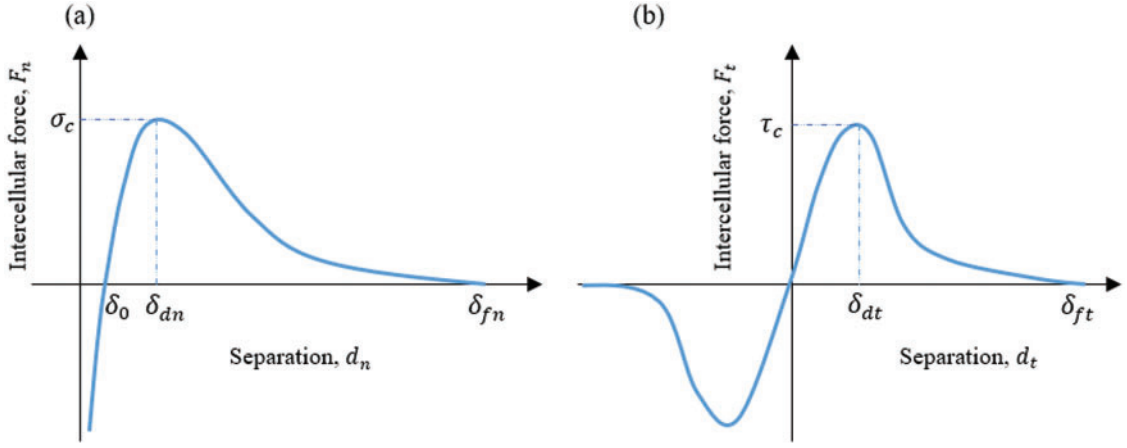

Figure 3: Intercellular interactions at cell-cell junction: (a) Normal direction, (b) Tangential direction

2.2.2 Cell-Substrate Adhesion Modeling

Cell movement also invloves cell-substrate adhesion which is the attachement of a cell to the underlying substrate through mechanosensitive focal adhesion complexes of the integrin family [57]. It enables cell activity in the extracellular matrix to affect the cell shape and movement. There have been many efforts on the modeling of cell–substrate interactions [58–61]. An exponential cohesive zone model [62] was employed to represent the cell–substrate interfacial behavior [60]. The normal traction of the cell–substrate adhesion can be ignored according to previous analysis [63]. Therefore, we only consider the cell–substrate adhesive traction in xy plane for simplification in this study, and it takes the following form:

$$F_{c-s} = \begin{cases} \tau_{c-s}\left(\dfrac{d_u}{\delta_{du}}\right) e^{\dfrac{1}{2}-\dfrac{d_u^2}{2\delta_{du}^2}} & 0 \le |d_u| \le \delta_{du} \\ \tau_{c-s}\dfrac{d_u}{|d_u|}\left(\dfrac{\delta_f - |d_u|}{\delta_f - \delta_{du}}\right)^{p_t} & \delta_{du} \le |d_u| \le \delta_f \\ 0 & other \end{cases} \tag{3}$$

In the above equation, τ_{c-s} represents the maximum cell-substrate adhesion strength. In this study, τ_{c-s} was set to be 5 Pa according to the previous experimental measurement [63]. The d_u is the separation distance between the cell and the substrate. The critical interaction distance δ_{du} is the distance between the cell and the substrate when cell-substrate adhesion reaches its maximum value, which was set to be 25 nm according to previous study [60]. The detachment distance δ_f is estimated as 60 nm according to the reported measurements [64,65].

2.2.3 Protrusion Force Modeling

In the protrusion-based cell migration, actin polymerization leads to the formation of protrusions that adhere to the surrounding extracellular matrix (ECM). Then the formed protrusions retract, resulting in cell movement along the cell path [66,67]. Cell migration is a dynamic process

that is highly regulated by complex biological cues [68]. The formation of protrusion generates protrusion forces at the leading edge of the motile cell that could empower cell movement. The value of traction force on leading edge ranges from 0.25 to 3 nN according to the previous experimental studies depending on different measurement methods [69,70]. In addition, it is shown that each cell in an advancing epithelial monolayer was also involved in a global tug-of-war [63]. Therefore, in this study, one cell located at far left of the box was selected as the motile cell (Fig. 1), and a 2 nN protrusion force was applied on the motile cell along the x-axis direction. The protrusion forces on edges of all other cells were applied along random directions in the range of 0–0.3 nN.

2.3 Material Properties

In this study, the epithelial cell was assumed as an isotropic elastic material and the Young's modulus was set at different values between 0.3 and 30 KPa, and Poisson's ratio $\nu = 0.45$ according to the measurements reported in previous experiments [71,72]. The mass density was set to be 2×10^{-3} ng/μm^3 for individual epithelial cell according to the previous measurements [73,74]. In the curent cell modeling, we did not model the detailed cell internal microstructures.

3 Finite Element Implementation

In this study, a displacement-based finite element formulation was developed. The Galerkin weak formulation of the compuational model that neglects the body force during the deformation can be represented by the following terms:

$$\int_{\Omega} \rho \ddot{\mathbf{u}} \cdot \delta \mathbf{u} d\Omega = \int_{S_{ext}} \mathbf{T}^{p} \cdot \delta \mathbf{u} dS + \int_{S_{c-c}} \mathbf{T}^{c-c} \cdot \delta \Delta dS + \int_{S_{c-s}} \mathbf{T}^{c-s} \cdot \delta \mathbf{u} dS - \int_{\Omega} \mathbf{P} : \delta \mathbf{F} d\Omega \tag{4}$$

where ρ is the material density of the cell, Ω is the volume, S_{ext} is the cell external surface, S_{c-c} is the cell-cell junction surface, S_{c-s} is the cell-substrate surface. $\mathbf{T}^{p}$ is the protrusion traction vector, $\mathbf{T}^{c-c}$ and $\mathbf{T}^{c-s}$ are the intercellular interaction traction vector and cell-substrate interaction traction vector, respectively, $\mathbf{P}$ is the first Piola-Kirchhoff stress tensor, and $\mathbf{P} : \delta \mathbf{F} = P^{ij} \delta F_{ji}$. The descrete equations of motion can be expressed by following forms:

$$\mathbf{M}\ddot{\mathbf{u}} = \mathbf{F}_{ext} - \mathbf{F}_{int} \tag{5}$$

$$\mathbf{F}_{ext} = \mathbf{F}^{p} + \mathbf{F}^{c-c} + \mathbf{F}^{c-s} \tag{6}$$

In the above equations, $\mathbf{M}$ is the mass matrix, $\mathbf{F}_{ext}$ is external force which is consitituted of protrusion force $\mathbf{F}^{p}$, intercellular interaction force $\mathbf{F}^{c-c}$ and cell-substrate adhesion force $\mathbf{F}^{c-s}$. $\mathbf{F}_{int}$ represent the internal force resulting from the epithelial cell deformation.

4 Simulation Results

Numerical simulations were performed to investigate the cell migration behavior in a confluent epithelial monolayer. All simulations were conducted by using a custom-designed finite element package using Fortran, which was developed by Lin et al. [42].

4.1 Stress Distribution in Epithelial Monolayer Sheet

In the finite element simulation, each cell in the monolayer sheet was discretized into linear triangle elements to perform the computation. At each nodal point, the maximum and minimum

principal stresses were calculated according to the following formulation:

$$\sigma_{max} = \frac{\sigma_{xx} + \sigma_{yy}}{2} + \sqrt{\left(\frac{\sigma_{xx} - \sigma_{yy}}{2}\right)^2 + \tau_{xy}^2} \tag{7}$$

$$\sigma_{min} = \frac{\sigma_{xx} + \sigma_{yy}}{2} - \sqrt{\left(\frac{\sigma_{xx} - \sigma_{yy}}{2}\right)^2 + \tau_{xy}^2} \tag{8}$$

Then the average local normal stress is computed as $\sigma_{ave} = (\sigma_{max} + \sigma_{min})/2$ and the maximum shear stress is computed as $\tau_{max} = (\sigma_{max} - \sigma_{min})/2$. Fig. 4 shows the contours of the average local normal stress and the maximum shear stress while the motile cell migrates from the left to right with cell stiffness of 0.3 KPa. It can be seen that the value of the average local normal stress is greater than the value of the maximum shear stress in the motile cell. These observations were consistent with experimental studies [54,75], some other studies reported comparable amount of shear stress obtained through experiments [51,63]. To visualize the entire migration process, one cell located at far left of the box was selected as the motile cell. The motile cell migration in the monolayer can be seen in movie S1. All other cells are migrating with very small displacement compared to the motile cell since the protrusion force applied on the motile cell is larger than the rest of the cells. In our current study, the cell extrusion is not considered. When the maximum stress in the cell monolayer reached a predefined threshold value, cell remodeling will start and cells will change their shapes during the migration process. Cells may change their neighbors after cell remodeling. The cell density is maintained during the collective cell migration process.

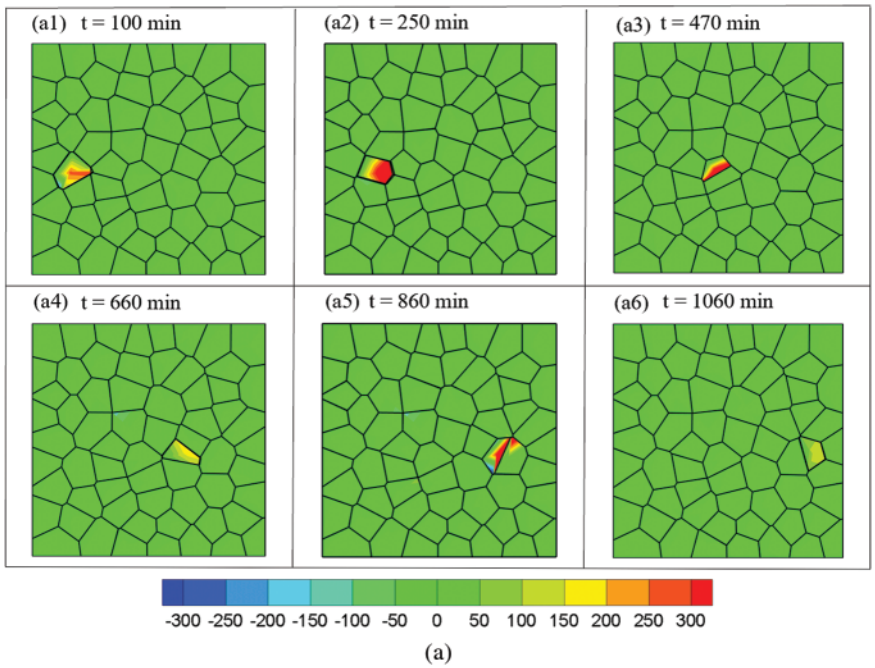

Figure 4: (Continued)

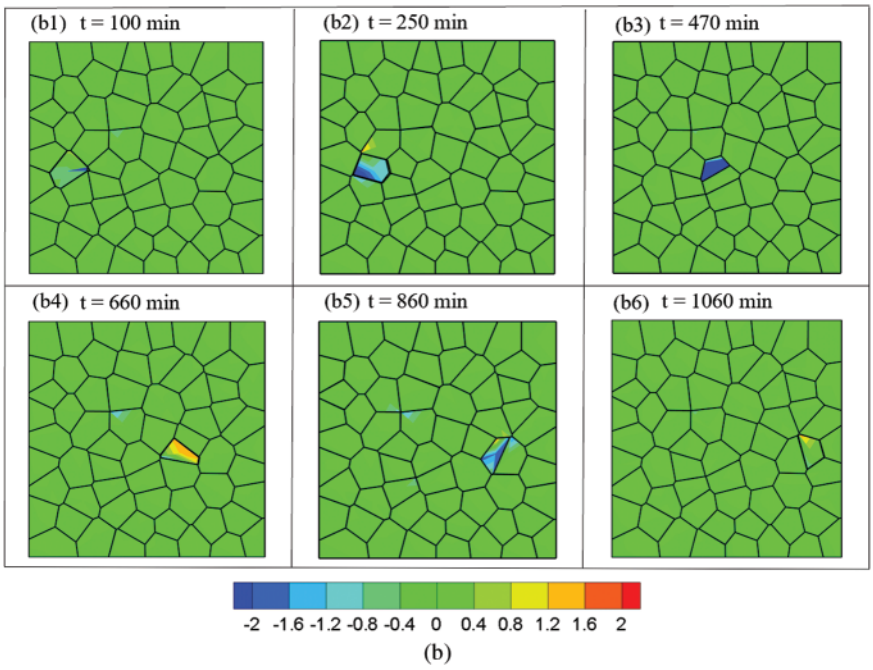

Figure 4: Stress distribution at different time step while the motile cell migrates from left to right: (a) Contour of average normal stress and (b) Contour of average shear stress at different time step: t = 100 min, t = 250 min, t = 470 min, t = 660 min, t = 860 min, t = 1060 min

Then we plot the effective stress in the epithelial monolayer sheet in Fig. 5. It can be seen that the stress in the motile cell is several orders higher than stress in other cells.

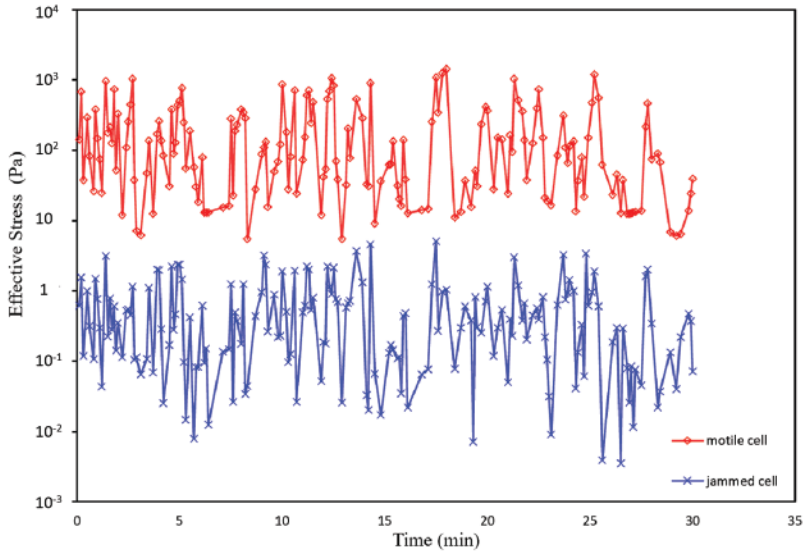

Figure 5: Effective stress in the motile cell and the jammed cell

4.2 Contribution of the Cell Stiffness on Cell Migration Behavior

Cell stiffness has been identified as an important mechanical property that influences cell motility and cell migration behavior. Many experimental studies have shown that higher cell motility often relates to lower stiffness, which might favor cell migration, epithelial-mesenchymal transition in many biological activities [25,26,76–79]. However, some conflicting evidence has been reported that cancerous cells with higher motility are stiffer than their benign counterparts [80,81] that makes the relationship between cell stiffness and cell motility still a controversial topic. The value of epithelial cell stiffness has been reported in a range from 0.1 to 20 KPa depending on different cell types and measurements [72,82]. To computationally explore the effects of cell stiffness on the cell migration behavior, in this study, all the parameters were kept the same except the stiffness was set to be 0.3, 3, 10, 20 KPa respectively for different cases. The displacement of the motile cell verses time during the migration is plotted in Fig. 6. It can be seen that higher stiffness results in smaller displacement and lower migration speed. This result is consistent with previous studies [25,26,76–79] since low cell stiffness often associated with higher ability to deform, therefore leads to higher motility.

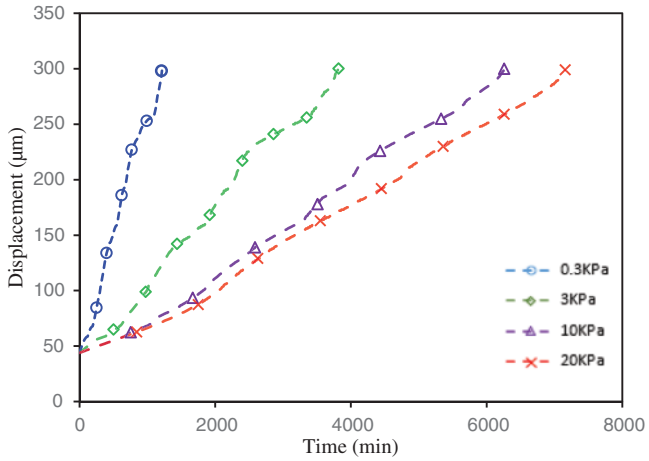

Figure 6: Displacement of the motile cell during the migration processes with different cell stiffness

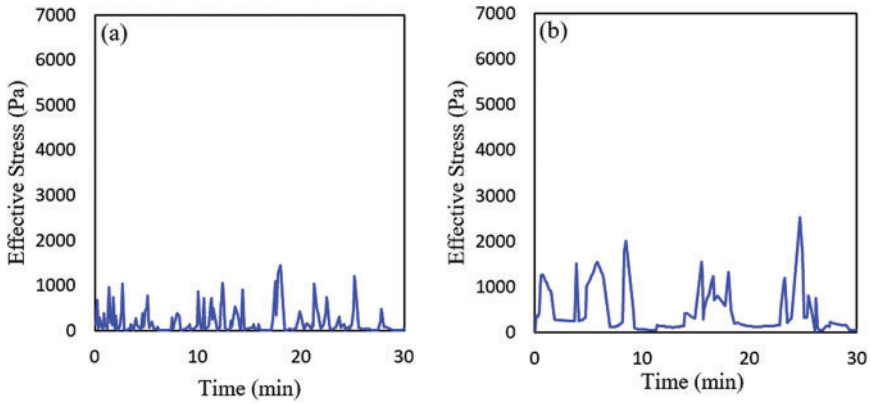

Figure 7: (Continued)

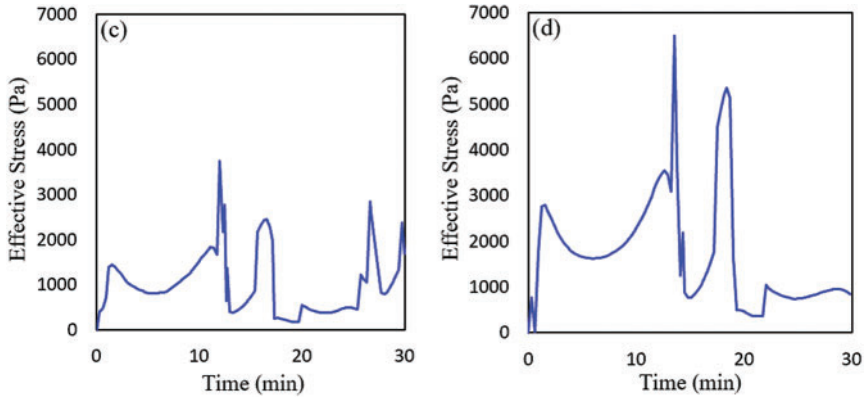

Figure 7: Effective stress *vs.* time in the motile cell with differnet cell stiffness: (a) E = 0.3 KPa, (b) E = 3 KPa, (c) E = 10 KPa, (d) E = 20 KPa

Then we plotted the effective stress in the motile cell during the cell migration for all four cases with different cell stiffness as shown in Fig. 7. One might see that higher stiffness leads to higher stress in the cell which is consistent with recent experimental studies [27,83,84].

5 Discussions and Conclusions

In this study, a continuum physics-based computational model including the intercellular interaction was employed to study the cell migration behavior in a confluent epithelial monolayer. The epithelial layer was modeled as an isotropic elastic material. Through finite element simulation, the results revealed that the motile cell was subjected to higher stress than other cells during the migration process. And our results showed that the normal intercellular interaction dominates over the tangential intercellular interaction. Cell stiffness was indicated to play a significant role in cell migration behavior, higher stiffness results in smaller displacement and lower migration speed. When transiting from the quiescent state to the motile state, the traction force in epithelial cell may decrease in order to escape from the collective cells. The simulation model-based study may provide possible explanations and insights on how the mechanical cues affect the cell migration behavior.

It should be noted that cell migration is a complex biological phenomenon, and there are several limitations associated with the presented study. Firstly, a 2D plane stress model was used for simplification in this study, which might not fully represent the 3D cases. Secondly, the epithelial cells were modelled as the simple isotropic material which does not consider the detailed cell microstructure and the complex cell material properties. Thirdly, the presented computational model does not take into account of the factors such as "chemotaxis" or "durotaxis" in cell movements, so the protrusion force applied may not be realistic in real situation. Only one cell is selected as motile cell in the current study. In our previous cell migration study, we investigate how the number of self-propelled monocytes affected the collective migration behavior as a group. It was found that more self-propelled cells are in the system moving along the same direction, the faster the collective group migrates toward coordinated direction [85]. In our future study, we plan to build cell model with internal microstructures by using liquid crystal and liquid crystal elastomers, and to build a 3D epithelial cell migration model to further investigate the role of mechanical interaction on the cell migration behaviors.

Funding Statement: This work is supported by a grant from National Institutes of Health (Grant No. SC2GM112575) and a grant from the John L. Santikos Charitable Foundation of the San Antonio Area Foundation.

Conflicts of Interest: The authors declare that they have no conflicts of interest to report regarding the present study.

References

1. Aman, A., Piotrowski, T. (2010). Cell migration during morphogenesis. *Developmental Biology, 341(1),* 20–33. DOI 10.1016/j.ydbio.2009.11.014.
2. Haage, A., Wagner, K., Deng, W., Venkatesh, B., Mitchell, C. et al. (2020). Precise coordination of cell-ECM adhesion is essential for efficient melanoblast migration during development. *Development, 147(14),* dev184234. DOI 10.1242/dev.184234.
3. Mongera, A., Rowghanian, P., Gustafson, H. J., Shelton, E., Kealhofer, D. A. et al. (2018). A fluid-to-solid jamming transition underlies vertebrate body axis elongation. *Nature, 561(7723),* 401–405. DOI 10.1038/s41586-018-0479-2.
4. Saykali, B., Mathiah, N., Nahaboo, W., Racu, M. L., Hammou, L. et al. (2019). Distinct mesoderm migration phenotypes in extra-embryonic and embryonic regions of the early mouse embryo. *Elife, 8,* e42434. DOI 10.7554/eLife.42434.001.
5. Dekoninck, S., Blanpain, C. (2019). Stem cell dynamics, migration and plasticity during wound healing. *Nature Cell Biology, 21(1),* 18–24. DOI 10.1038/s41556-018-0237-6.
6. Li, L., He, Y., Zhao, M., Jiang, J. (2013). Collective cell migration: Implications for wound healing and cancer invasion. *Burns & Trauma, 1(1),* 2321–3868. DOI 10.4103/2321-3868.113331.
7. Xiao, Y., Riahi, R., Torab, P., Zhang, D. D., Wong, P. K. (2019). Collective cell migration in 3D epithelial wound healing. *ACS Nano, 13(2),* 1204–1212. DOI 10.1021/acsnano.8b06305.
8. Campbell, K., Rossi, F., Adams, J., Pitsidianaki, I., Barriga, F. M. et al. (2019). Collective cell migration and metastases induced by an epithelial-to-mesenchymal transition in drosophila intestinal tumors. *Nature Communications, 10(1),* 1–10. DOI 10.1038/s41467-019-10269-y.
9. Clark, A. G., Vignjevic, D. M. (2015). Modes of cancer cell invasion and the role of the microenvironment. *Current Opinion in Cell Biology, 36,* 13–22. DOI 10.1016/j.ceb.2015.06.004.
10. Miyazaki, K., Oyanagi, J., Hoshino, D., Togo, S., Kumagai, H. et al. (2019). Cancer cell migration on elongate protrusions of fibroblasts in collagen matrix. *Scientific Reports, 9(1),* 1–15. DOI 10.1038/s41598-018-36646-z.
11. Paul, C. D., Mistriotis, P., Konstantopoulos, K. (2017). Cancer cell motility: Lessons from migration in confined spaces. *Nature Reviews Cancer, 17(2),* 131–140. DOI 10.1038/nrc.2016.123.
12. Collins, C., Nelson, W. J. (2015). Running with neighbors: Coordinating cell migration and cell-cell adhesion. *Current Opinion in Cell Biology, 36,* 62–70. DOI 10.1016/j.ceb.2015.07.004.
13. Friedl, P., Gilmour, D. (2009). Collective cell migration in morphogenesis, regeneration and cancer. *Nature Reviews Molecular Cell Biology, 10(7),* 445–457. DOI 10.1038/nrm2720.
14. Kabla, A. J. (2012). Collective cell migration: Leadership, invasion and segregation. *Journal of the Royal Society Interface, 9(77),* 3268–3278. DOI 10.1098/rsif.2012.0448.
15. Cowin, S. C., Doty, S. B. (2007). *Tissue mechanics.* New York: Springer.
16. Park, J. A., Kim, J. H., Bi, D., Mitchel, J. A., Qazvini, N. T. et al. (2015). Unjamming and cell shape in the asthmatic airway epithelium. *Nature Materials, 14(10),* 1040–1048. DOI 10.1038/nmat4357.
17. Park, J. A., Atia, L., Mitchel, J. A., Fredberg, J. J., Butler, J. P. (2016). Collective migration and cell jamming in asthma, cancer and development. *Journal of Cell Science, 129(18),* 3375–3383. DOI 10.1242/jcs.187922.
18. Mitchel, J. A., Das, A., O'Sullivan, M. J., Stancil, I. T., DeCamp, S. J. et al. (2020). In primary airway epithelial cells, the unjamming transition is distinct from the epithelial-to-mesenchymal transition. *Nature Communications, 11(1),* 1–14. DOI 10.1038/s41467-020-18841-7.

19. Oswald, L., Grosser, S., Smith, D. M., Käs, J. A. (2017). Jamming transitions in cancer. *Journal of Physics D: Applied Physics, 50(48),* 483001. DOI 10.1088/1361-6463/aa8e83.
20. Bronsert, P., Enderle-Ammour, K., Bader, M., Timme, S., Kuehs, M. et al. (2014). Cancer cell invasion and EMT marker expression: A three-dimensional study of the human cancer–host interface. *The Journal of Pathology, 234(3),* 410–422. DOI 10.1002/path.4416.
21. Ellison, D., Mugler, A., Brennan, M. D., Lee, S. H., Huebner, R. J. et al. (2016). Cell–cell communication enhances the capacity of cell ensembles to sense shallow gradients during morphogenesis. *Proceedings of the National Academy of Sciences, 113(6),* E679–E688. DOI 10.1073/pnas.1516503113.
22. Hava, D., Forster, U., Matsuda, M., Cui, S., Link, B. A. et al. (2009). Apical membrane maturation and cellular rosette formation during morphogenesis of the zebrafish lateral line. *Journal of Cell Science, 122(5),* 687–695. DOI 10.1242/jcs.032102.
23. Garcia, S., Hannezo, E., Elgeti, J., Joanny, J. F., Silberzan, P. et al. (2015). Physics of active jamming during collective cellular motion in a monolayer. *Proceedings of the National Academy of Sciences, 112(50),* 15314–15319. DOI 10.1073/pnas.1510973112.
24. Bazellières, E., Conte, V., Elosegui-Artola, A., Serra-Picamal, X., Bintanel-Morcillo, M. et al. (2015). Control of cell–cell forces and collective cell dynamics by the intercellular adhesome. *Nature Cell Biology, 17(4),* 409–420. DOI 10.1038/ncb3135.
25. Raudenska, M., Kratochvilova, M., Vicar, T., Gumulec, J., Balvan, J. et al. (2019). Cisplatin enhances cell stiffness and decreases invasiveness rate in prostate cancer cells by actin accumulation. *Scientific Reports, 9(1),* 1–11. DOI 10.1038/s41598-018-38199-7.
26. Luo, Q., Kuang, D., Zhang, B., Song, G. (2016). Cell stiffness determined by atomic force microscopy and its correlation with cell motility. *Biochimica et Biophysica Acta (BBA)-General Subjects, 1860(9),* 1953–1960. DOI 10.1016/j.bbagen.2016.06.010.
27. Lin, H. H., Lin, H. K., Lin, I. H., Chiou, Y. W., Chen, H. W. et al. (2015). Mechanical phenotype of cancer cells: Cell softening and loss of stiffness sensing. *Oncotarget, 6(25),* 20946. DOI 10.18632/oncotarget.4173.
28. Glazier, J. A., Graner, F. (1993). Simulation of the differential adhesion driven rearrangement of biological cells. *Physical Review E, 47(3),* 2128. DOI 10.1103/physreve.47.2128.
29. Graner, F., Glazier, J. A. (1992). Simulation of biological cell sorting using a two-dimensional extended potts model. *Physical Review Letters, 69(13),* 2013. DOI 10.1103/PhysRevLett.69.2013.
30. Swat, M. H., Thomas, G. L., Belmonte, J. M., Shirinifard, A., Hmeljak, D. et al. (2012). Multi-scale modeling of tissues using CompuCell3d. *Methods in Cell Biology, 110,* 325–366. DOI 10.1016/B978-0-12-388403-9.00013-8.
31. Szabó, A., Merks, R. M. (2013). Cellular potts modeling of tumor growth, tumor invasion, and tumor evolution. *Frontiers in Oncology, 3,* 87. DOI 10.3389/fonc.2013.00087.
32. George, M., Bullo, F., Campàs, O. (2017). Connecting individual to collective cell migration. *Scientific Reports, 7(1),* 1–10. DOI 10.1038/s41598-017-10069-8.
33. Smeets, B., Alert, R., Pešek, J., Pagonabarraga, I., Ramon, H. et al. (2016). Emergent structures and dynamics of cell colonies by contact inhibition of locomotion. *Proceedings of the National Academy of Sciences, 113(51),* 14621–14626. DOI 10.1073/pnas.1521151113.
34. Woods, M. L., Carmona-Fontaine, C., Barnes, C. P., Couzin, I. D., Mayor, R. et al. (2014). Directional collective cell migration emerges as a property of cell interactions. *PLoS One, 9(9),* e104969. DOI 10.1371/journal.pone.0104969.
35. Bi, D., Lopez, J. H., Schwarz, J. M., Manning, M. L. (2015). A density-independent rigidity transition in biological tissues. *Nature Physics, 11(12),* 1074–1079. DOI 10.1038/nphys3471.
36. Bi, D., Lopez, J. H., Schwarz, J. M., Manning, M. L. (2014). Energy barriers and cell migration in densely packed tissues. *Soft Matter, 10(12),* 1885–1890. DOI 10.1039/C3SM52893F.
37. Bi, D., Yang, X., Marchetti, M. C., Manning, M. L. (2016). Motility-driven glass and jamming transitions in biological tissues. *Physical Review X, 6(2),* 021011. DOI 10.1103/PhysRevX.6.021011.
38. Giavazzi, F., Paoluzzi, M., Macchi, M., Bi, D., Scita, G. et al. (2018). Flocking transitions in confluent tissues. *Soft Matter, 14(18),* 3471–3477. DOI 10.1039/C8SM00126J.

39. Li, B., Sun, S. X. (2014). Coherent motions in confluent cell monolayer sheets. *Biophysical Journal, 107(7),* 1532–1541. DOI 10.1016/j.bpj.2014.08.006.
40. Chen, H. H., Brodland, G. W. (2000). Cell-level finite element studies of viscous cells in planar aggregates. *Journal of Biomechanical Engineering., 122(4),* 394–401. DOI 10.1115/1.1286563.
41. Brodland, G. W., Viens, D., Veldhuis, J. H. (2007). A new cell-based FE model for the mechanics of embryonic epithelia. *Computer Methods in Biomechanics and Biomedical Engineering, 10(2),* 121–128. DOI 10.1080/10255840601124704.
42. Lin, L., Zeng, X. (2018). Numerical investigation of the role of intercellular interactions on collective epithelial cell migration. *Biomechanics and Modeling in Mechanobiology, 17(2),* 439–448. DOI 10.1007/s10237-017-0970-y.
43. Lee, A. J., Hugonnet, H., Park, W., Park, Y. (2020). Three-dimensional label-free imaging and quantification of migrating cells during wound healing. *Biomedical Optics Express, 11(12),* 6812–6824. DOI 10.1364/BOE.405087.
44. Dörschel, B., Hermsdorf, D., Pieck, S., Starke, S., Thiele, H. (2002). Thickness measurements on cell monolayers using CR-39 detectors. *Nuclear Instruments and Methods in Physics Research Section B: Beam Interactions with Materials and Atoms, 187(4),* 525–534. DOI 10.1016/S0168-583X(01)01148-X.
45. Lin, L., Wang, X., Zeng, X. (2014). Geometrical modeling of cell division and cell remodeling based on Voronoi tessellation method. *Computer Modeling in Engineering & Sciences, 98(2),* 203–220. DOI 10.3970/cmes.2014.098.203.
46. González-Valverde, I., García-Aznar, J. M. (2019). An agent-based and FE approach to simulate cell jamming and collective motion in epithelial layers. *Computational Particle Mechanics, 6(1),* 85–96. DOI 10.1007/s40571-018-0199-2.
47. De Paiva, C. S., Pflugfelder, S. C., Li, D. Q. (2006). Cell size correlates with phenotype and proliferative capacity in human corneal epithelial cells. *Stem Cells, 24(2),* 368–375. DOI 10.1634/stemcells.2005-0148.
48. Kaufmann, R., Piontek, J., Grüll, F., Kirchgessner, M., Rossa, J. et al. (2012). Visualization and quantitative analysis of reconstituted tight junctions using localization microscopy. *PLoS One, 7(2),* e31128. DOI 10.1371/journal.pone.0031128.
49. Giepmans, B. N., van Ijzendoorn, S. C. (2009). Epithelial cell–cell junctions and plasma membrane domains. *Biochimica et Biophysica Acta (BBA)-Biomembranes, 1788(4),* 820–831. DOI 10.1016/j.bbamem.2008.07.015.
50. Vedula, S. R. K., Ravasio, A., Lim, C. T., Ladoux, B. (2013). Collective cell migration: A mechanistic perspective. *Physiology, 28(6),* 370–379. DOI 10.1152/physiol.00033.2013.
51. Patel, N. G., Nguyen, A., Xu, N., Ananthasekar, S., Alvarez, D. F. et al. (2020). Unleashing shear: Role of intercellular traction and cellular moments in collective cell migration. *Biochemical and Biophysical Research Communications, 522(2),* 279–285. DOI 10.1016/j.bbrc.2019.11.048.
52. Wang, X. H., Yang, F., Pan, J. B., Kang, B., Xu, J. J. et al. (2020). Quantitative imaging of pN intercellular force and energetic costs during collective cell migration in epithelial wound healing. *Analytical Chemistry, 92(24),* 16180–16187. DOI 10.1021/acs.analchem.0c03935.
53. Cho, Y., Son, M., Jeong, H., Shin, J. H. (2018). Electric field–induced migration and intercellular stress alignment in a collective epithelial monolayer. *Molecular Biology of the Cell, 29(19),* 2292–2302. DOI 10.1091/mbc.E18-01-0077.
54. Tambe, D. T., Hardin, C. C., Angelini, T. E., Rajendran, K., Park, C. Y. et al. (2011). Collective cell guidance by cooperative intercellular forces. *Nature Materials, 10(6),* 469–475. DOI 10.1038/nmat3025.
55. Lin, L., Samuel, J., Zeng, X., Wang, X. (2017). Contribution of extrafibrillar matrix to the mechanical behavior of bone using a novel cohesive finite element model. *Journal of the Mechanical Behavior of Biomedical Materials, 65,* 224–235. DOI 10.1016/j.jmbbm.2016.08.027.
56. Liu, Z., Tan, J. L., Cohen, D. M., Yang, M. T., Sniadecki, N. J. et al. (2010). Mechanical tugging force regulates the size of cell–cell junctions. *Proceedings of the National Academy of Sciences, 107(22),* 9944–9949. DOI 10.1073/pnas.0914547107.

57. Paddillaya, N., Mishra, A., Kondaiah, P., Pullarkat, P., Menon, G. I. et al. (2019). Biophysics of cell-substrate interactions under shear. *Frontiers in Cell and Developmental Biology, 7,* 251. DOI 10.3389/fcell.2019.00251.
58. Ziebert, F., Aranson, I. S. (2016). Computational approaches to substrate-based cell motility. *npj Computational Materials, 2(1),* 1–16. DOI 10.1038/npjcompumats.2016.19.
59. Roy, S., Qi, H. J. (2010). A computational biomimetic study of cell crawling. *Biomechanics and Modeling in Mechanobiology, 9(5),* 573–581. DOI 10.1007/s10237-010-0198-6.
60. McGarry, J. P., Murphy, B. P., McHugh, P. E. (2005). Computational mechanics modelling of cell–substrate contact during cyclic substrate deformation. *Journal of the Mechanics and Physics of Solids, 53(12),* 2597–2637. DOI 10.1016/j.jmps.2005.07.006.
61. Vernerey, F. J., Farsad, M. (2014). A mathematical model of the coupled mechanisms of cell adhesion, contraction and spreading. *Journal of Mathematical Biology, 68(4),* 989–1022. DOI 10.1007/s00285-013-0656-8.
62. Xu, X. P., Needleman, A. (1994). Numerical simulations of fast crack growth in brittle solids. *Journal of the Mechanics and Physics of Solids, 42(9),* 1397–1434. DOI 10.1016/0022-5096(94)90003-5.
63. Trepat, X., Wasserman, M. R., Angelini, T. E., Millet, E., Weitz, D. A. et al. (2009). Physical forces during collective cell migration. *Nature Physics, 5(6),* 426–430. DOI 10.1038/nphys1269.
64. Saez, A., Anon, E., Ghibaudo, M., du Roure, O., di Meglio, J. M. et al. (2010). Traction forces exerted by epithelial cell sheets. *Journal of Physics: Condensed Matter, 22(19),* 194119. DOI 10.1088/0953-8984/22/19/194119.
65. Schoen, I., Hu, W., Klotzsch, E., Vogel, V. (2010). Probing cellular traction forces by micropillar arrays: Contribution of substrate warping to pillar deflection. *Nano Letters, 10(5),* 1823–1830. DOI 10.1021/nl100533c.
66. Gagliardi, P. A., Puliafito, A., di Blasio, L., Chianale, F., Somale, D. et al. (2015). Real-time monitoring of cell protrusion dynamics by impedance responses. *Scientific Reports, 5(1),* 1–12. DOI 10.1038/srep10206.
67. Devreotes, P., Horwitz, A. R. (2015). Signaling networks that regulate cell migration. *Cold Spring Harbor Perspectives in Biology, 7(8),* a005959. DOI 10.1101/cshperspect.a005959.
68. Whitelaw, J. A., Swaminathan, K., Kage, F., Machesky, L. M. (2020). The WAVE regulatory complex is required to balance protrusion and adhesion in migration. *Cells, 9(7),* 1635. DOI 10.3390/cells9071635.
69. Du Roure, O., Saez, A., Buguin, A., Austin, R. H., Chavrier, P. et al. (2005). Force mapping in epithelial cell migration. *Proceedings of the National Academy of Sciences of the United States of America, 102(7),* 2390–2395. DOI 10.1073/pnas.0408482102.
70. Gou, X., Yang, H., Fahmy, T. M., Wang, Y., Sun, D. (2014). Direct measurement of cell protrusion force utilizing a robot-aided cell manipulation system with optical tweezers for cell migration control. *The International Journal of Robotics Research, 33(14),* 1782–1792. DOI 10.1177/0278364914546536.
71. Berdyyeva, T. K., Woodworth, C. D., Sokolov, I. (2004). Human epithelial cells increase their rigidity with ageing *in vitro*: Direct measurements. *Physics in Medicine & Biology, 50(1),* 81. DOI 10.1088/0031-9155/50/1/007.
72. Guz, N., Dokukin, M., Kalaparthi, V., Sokolov, I. (2014). If cell mechanics can be described by elastic modulus: Study of different models and probes used in indentation experiments. *Biophysical Journal, 107(3),* 564–575. DOI 10.1016/j.bpj.2014.06.033.
73. Anaya-Hernández, A., Rodríguez-Castelán, J., Nicolás, L., Martínez-Gómez, M., Jiménez-Estrada, I. et al. (2015). Hypothyroidism affects differentially the cell size of epithelial cells among oviductal regions of rabbits. *Reproduction in Domestic Animals, 50(1),* 104–111. DOI 10.1111/rda.12455.
74. Park, K., Millet, L. J., Kim, N., Li, H., Jin, X. et al. (2010). Measurement of adherent cell mass and growth. *Proceedings of the National Academy of Sciences, 107(48),* 20691–20696. DOI 10.1073/pnas.1011365107.
75. Vishwakarma, M., Di Russo, J., Probst, D., Schwarz, U. S., Das, T. et al. (2018). Mechanical interactions among followers determine the emergence of leaders in migrating epithelial cell collectives. *Nature Communications, 9(1),* 1–12. DOI 10.1038/s41467-018-05927-6.
76. Cross, S. E., Jin, Y. S., Rao, J., Gimzewski, J. K. (2007). Nanomechanical analysis of cells from cancer patients. *Nature Nanotechnology, 2(12),* 780–783. DOI 10.1038/nnano.2007.388.

77. Suresh, S. (2007). Biomechanics and biophysics of cancer cells. *Acta Materialia, 55(12),* 3989–4014. DOI 10.1016/j.actbio.2007.04.002.
78. Zou, C., Luo, Q., Qin, J., Shi, Y., Yang, L. et al. (2013). Osteopontin promotes mesenchymal stem cell migration and lessens cell stiffness via integrin β1, FAK, and ERK pathways. *Cell Biochemistry and Biophysics, 65(3),* 455–462. DOI 10.1007/s12013-012-9449-8.
79. Mihai, C., Bao, S., Lai, J. P., Ghadiali, S. N., Knoell, D. L. (2012). PTEN inhibition improves wound healing in lung epithelia through changes in cellular mechanics that enhance migration. *American Journal of Physiology-Lung Cellular and Molecular Physiology, 302(3),* L287–L299. DOI 10.1152/ajplung.00037.2011.
80. Rathje, L. S. Z., Nordgren, N., Pettersson, T., Rönnlund, D., Widengren, J. et al. (2014). Oncogenes induce a vimentin filament collapse mediated by HDAC6 that is linked to cell stiffness. *Proceedings of the National Academy of Sciences, 111(4),* 1515–1520. DOI 10.1073/pnas.1300238111.
81. Bastatas, L., Martinez-Marin, D., Matthews, J., Hashem, J., Lee, Y. J. et al. (2012). AFM nano-mechanics and calcium dynamics of prostate cancer cells with distinct metastatic potential. *Biochimica et Biophysica Acta (BBA)-General Subjects, 1820(7),* 1111–1120. DOI 10.1016/j.bbagen.2012.02.006.
82. Wagh, A. A., Roan, E., Chapman, K. E., Desai, L. P., Rendon, D. A. et al. (2008). Localized elasticity measured in epithelial cells migrating at a wound edge using atomic force microscopy. *American Journal of Physiology-Lung Cellular and Molecular Physiology, 295(1),* L54–L60. DOI 10.1152/ajplung.00475.2007.
83. Beliveau, A., Thomas, G., Gong, J., Wen, Q., Jain, A. (2016). Aligned nanotopography promotes a migratory state in glioblastoma multiforme tumor cells. *Scientific Reports, 6(1),* 1–13. DOI 10.1038/srep26143.
84. Kraning-Rush, C. M., Califano, J. P., Reinhart-King, C. A. (2012). Cellular traction stresses increase with increasing metastatic potential. *PLoS One, 7(2),* e32572. DOI 10.1371/journal.pone.0032572.
85. Bai, J., Lin, L., Zeng, X. (2019). Computational study of collective cell migration by meshfree method. *Computer Modeling in Engineering & Sciences, 121(3),* 787–800. DOI 10.32604/cmes.2019.07159.